Reductive Elimination of Organic Molecules from Palladium−Diphosphine Complexes

Erik Zuidema,[†] Piet W. N. M. van Leeuwen,[†,‡] and Carles Bo*[,‡,§]

Van't Hoff Institute for Molecular Sciences, University of Amsterdam, Nieuwe Achtergracht 166, 1018 WV Amsterdam, The Netherlands, Departament de Química Física i Inorgànica, Universitat Rovira i Virgili, Campus Sescelades, Marcel·lí Domingo s/n, 43007 Tarragona, Spain, and Catalan Intitute of Chemical Research, ICIQ, Avda. Països Catalans, s/n, 43007 Tarragona, Spain

Received February 17, 2005

The effects governing the rate of reductive elimination of dimethyl ether, acetonitrile, vinyl cyanide, and methyl ethanoate from palladium diphosphine complexes were studied by means of a density functional theory method. Energy barriers, computed as the difference in energy between the reactant and the corresponding transition state using $H_2P(CH_2)_2PH_2$ as model for diphosphine ligands, varied from 38 kcal mol^{-1} (dimethyl ether) to barrierless elimination of methyl ethanoate, in good agreement with experimental results. MO analysis reveals striking differences that are related to the donor/acceptor capabilities of the reacting moieties. For the elimination of acetonitrile, the bite angle effect on the reaction rate, observed by Moloy when different diphosphine ligands were used, was studied in depth. We considered $(R_2PXPR_2)Pd(CH_3)(CN)$ complexes for a number of different ligand backbones ($X = (CH_2)_n$, $n = 1-4$; X = *cis*-, *trans*-but-2-ene) which span a large bite angle range and for a number of different phosphine substituents (R = H, Me, Ph). With the use of QM/MM strategies, steric and electronic effects were separated and evaluated, and the results indicate that the rate enhancement is electronic in nature, steric effects being negligible. The analysis reveals that wide bite angle ligands destabilize the reactant and stabilize the transition state, thus accelerating the reaction.

1. Introduction

The reductive elimination reaction is the product-forming step in many transition-metal-catalyzed reactions. Formally, the metal reduces its oxidation state by two units while two metal−ligand bonds break and a new R_1-R_2 bond forms (Scheme 1). Examples of these reactions include industrially important processes such as palladium-catalyzed carbonylation, the Heck reaction,[1] and cross-coupling reactions,[2] such as the Suzuki coupling reaction,[3] and nickel-catalyzed hydrocyanation.[4]

Early studies focused on the formation of carbon−carbon and carbon−hydrogen bonds. The mechanism of reductive elimination of alkanes from palladium complexes, through either C−C or C−H bond formation, has been studied extensively, both experimentally[5,6] and theoretically.[7−12] In the last two decades the experimental scope of the reaction has been extended to reactions involving bond formation between differently hybridized carbon atoms. Furthermore, the formation of carbon−heteroatom bonds through reductive elimination has become a key step in the palladium-catalyzed production of esters, arylamines,[13] aryl ethers,[14] aryl sulfides, and arylphosphines.

Scheme 1

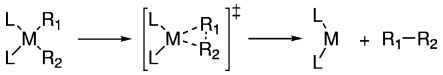

From experimental studies it is clear that the rate of the reductive elimination is highly dependent on the nature of the two reacting moieties and the noninnocent spectator ligands. For some reactions the reductive elimination proceeds readily even at low temperatures,

* To whom correspondence should be addressed. E-mail: cbo@iciq.es.
† University of Amsterdam.
‡ ICIQ.
§ Universitat Rovira i Virgili.

(1) Heck, R. F. J. *J. Am. Chem. Soc.* **1968**, *90*, 5518. Shibasaki, M.; Vogl, E. M. In *Comprehensive Asymmetric Catalysis*; Jacobsen, E. N., Pfaltz, A., Yamamoto, H., Eds.; Springer-Verlag: Berlin, Heidelberg, 1999.
(2) Farina, V. In *Comprehensive Organometallic Chemistry II*; Hegedus, L. S., Ed.; Pergamon: Oxford, U.K., 1995.
(3) Cornils, B.; Herrmann, W. A. *Applied Homogeneous Catalysis with Organometallic Compounds*, 2nd ed.; Wiley-VCH: Weinheim, Germany, 2002.
(4) Kranenburg, M.; Kamer, P. C. J.; van Leeuwen, P. W. N. M.; Vogt, D.; Keim, W. *J. Chem. Soc., Chem. Commun.* **1995**, 2177−2178.
(5) Gillie, A.; Stille, J. K. *J. Am. Chem. Soc.* **1980**, *102*, 4933−4941.
(6) Moravskiy, A.; Stille, J. K. *J. Am. Chem. Soc.* **1981**, *103*, 4182−4186.
(7) Tatsumi, K.; Hoffmann, R.; Yamamoto, A.; Stille, J. K. *Bull. Chem. Soc. Jpn.* **1981**, *54*, 1857−1867.
(8) Balazs, A. C.; Johnson, K. H.; Whitesides, G. M. *Inorg. Chem.* **1982**, *21*, 2162−2174.
(9) Low, J. J.; Goddard, W. A. *Organometallics* **1986**, *4*, 609−622.
(10) Low, J. J.; Goddard, W. A. *J. Am. Chem. Soc.* **1986**, *108*, 6115−6128.
(11) Calhorda, M. J.; Brown, J. M.; Cooley, N. A. *Organometallics* **1991**, *10*, 1431−1438.
(12) Dedieu, A. *Chem. Rev.* **2000**, *100*, 543−600.
(13) Driver, M. S.; Hartwig, J. F. *J. Am. Chem. Soc.* **1997**, *119*, 8232−8245.
(14) Mann, G.; Incarvito, C.; Rheingold, A. L.; Hartwig, J. F. *J. Am. Chem. Soc.* **1999**, *121*, 3224−3225.

10.1021/om050113x CCC: $30.25
Publication on Web 06/18/2005

while for other reactions elevated temperatures and prolonged reaction times are required. Surprisingly, theoretical and experimental studies that focus on the comparison of these different elimination reactions are scarce.[15] Instead, efforts have mainly been focused on the role of spectator ligands on the rate of elimination in individual reactions. The rate of the reductive elimination is influenced by both steric[16,17] and electronic[16−18] effects induced by auxiliary ligands coordinated to the metal. The steric effect is usually rationalized as a repulsive interaction between the spectator ligands and the two reacting moieties in the reactant complex, forcing the two species in close proximity and facilitating the elimination reaction. Rationalization of the electronic effect is less straightforward, but it has been shown that in the palladium-catalyzed C−C bond forming reactions, the rate of elimination is inversely proportional to the ligand basicity,[18] probably due to stabilization of the higher oxidation state of the metal center in the reactant.

When bidentate ligands are used, the natural bite angle seems to correlate with the rate of elimination.[19,20] In one example, Marcone and Moloy studied the reductive elimination of RCN from (diphosphine)Pd(R)(CN) for a number of electronically similar cis-coordinating diphosphine ligands and they found that the rate of elimination increases enormously as the natural bite angle of the ligand increases.[21] The origin of this bite angle effect in palladium diphosphine mediated reactions remains unclear. On the basis of literature data, we recently argued that the observed bite angle effect on the reductive elimination of a number of compounds from palladium diphosphine complexes is largely electronic in nature.[22] However, our arguments rely heavily on experimental studies, in which electronic and steric effects are intertwined and therefore difficult to study separately.

In contrast, theoretical studies have shown to be a powerful tool in identifying and understanding individual factors governing the rate and selectivity of transition-metal-catalyzed reactions. Early pioneering works[7−11] on the reductive elimination reaction have yielded valuable insights into $C_{sp^3}-C_{sp^3}$ and $C_{sp^3}-H$ bond formation. Only a few theoretical studies have been published that focus on C−C bond formation involving unsaturated substrates and C−heteroatom bond formation. In one of the few examples of reactions involving unsaturated substrates, Ananikov et al.[23] studied the formation of butadiene from transition-metal complexes containing different spectator ligands and showed that $C_{sp^2}-C_{sp^2}$ reductive elimination proceeds much more readily than $C_{sp^3}-C_{sp^3}$ elimination for both palladium and platinum diphosphine complexes. During the preparation of this paper, these authors reported[24] a comprehensive study on C−C coupling reactions of $(PH_3)_2MRR'$ (M = Pd, Pt) complexes and found a correlation between the M−R bond strengths, the activation energy for reductive elimination, the reaction exothermicity, and the directionality of the M−R bond, although they suggested some kind of steric interaction between R and the phosphine. Recently, Macgregor and co-workers[15] reported on the subject of carbon−heteroatom bond formation, comparing several different C_{sp^3}−heteroatom bond forming reactions involving group 10 $(PH_3)_2M(CH_3)(X)$ and explaining the observed differences in reactivity in terms of $M-CH_3/M-X$ bond strengths and geometric distortions in the transition state.

Here we report a computational investigation on the factors governing the reductive elimination reaction in a variety of palladium diphosphine complexes which span a broad range of ligands and substrates. To investigate the large differences in the rate of reductive elimination observed for different C−C and C−O bond forming reactions, the model systems $(H_2PCH_2CH_2PH_2)PdXY$ were considered. Keeping the metal and ligand moieties invariable, X and Y are a number of different reacting species. The reactions studied here include examples of $C_{sp^2}-C_{sp}$, $C_{sp^3}-C_{sp}$, $C_{sp^3}-O$, and $C_{sp^2}-O$ bond forming processes. Orbital analysis reveals striking differences between the systems, explaining the large differences in reactivity. In one of these reactions, the reductive elimination of acetonitrile from palladium diphosphine complexes, ligand effects were studied in detail. To assess the bite angle effect, DFT calculations were performed on Moloy's systems $(R_2PXPR_2)Pd(CH_3)(CN)$ for a number of different ligand backbones (X = $(CH_2)_n$, $n = 1-4$; X = *cis*-, *trans*-but-2-ene) which span a large bite angle range and for a number of different phosphine substituents (R = H, Me, Ph). Hybrid quantum mechanics/molecular mechanics (QM/MM) strategies were used to separate electronic and steric effects, which provided more insight into the nature of the rate enhancement effect observed by Moloy.

2. Computational Details

All DFT calculations were performed using the Amsterdam Density Functional (ADF2000.02) program developed by Baerends et al.[25,26] We used the local VWN[27] exchange-correlation potential with nonlocal Becke's exchange correction[28] and Perdew's correlation correction[29] (BP86). Relativistic corrections were introduced by scalar-relativistic zero-order regular approximation (ZORA).[30−32] A triple-ζ plus polarization basis set was used on all atoms. For non-hydrogen atoms a relativ-

(15) Macgregor, S. A.; Neave, G. W.; Smith, C. *Faraday Discuss.* **2003**, *124*, 111−127.
(16) Mann, G.; Baranano, D.; Hartwig, J. F.; Rheingold, A. L.; Guzei, I. A. *J. Am. Chem. Soc.* **1998**, *120*, 9205−9219.
(17) Mann, G.; Shelby, Q.; Roy, A. H.; Hartwig, J. F. *Organometallics* **2003**, *22*, 2775−2789.
(18) Negishi, E.; Takahashi, T.; Akiyoshi, K. *J. Organomet. Chem.* **1987**, *334*, 181−194.
(19) van Leeuwen, P. W. N. M.; Kamer, P. C. J.; Reek, J. N. H.; Dierkes, P. *Chem. Rev.* **2000**, *100*, 2741−2769.
(20) Brown, J. M.; Guiry, P. J. *Inorg. Chim. Acta* **1994**, *220*, 249−259.
(21) Marcone, J. E.; Moloy, K. G. *J. Am. Chem. Soc.* **1998**, *120*, 8527−8528.
(22) Freixa, Z.; van Leeuwen, P. W. N. M. *Dalton* **2003**, *10*, 1890.
(23) Ananikov, V. P.; Musaev, D. G.; Morokuma, K. *J. Am. Chem. Soc.* **2002**, *124*, 2839−2852.
(24) Ananikov, V. P.; Musaev, D. G.; Morokuma, K. *Organometallics* **2005**, *24*, 715.
(25) Velde, G. T.; Bickelhaupt, F. M.; Baerends, E. J.; Guerra, C. F.; van Gisbergen, S. J. A.; Snijders, J. G.; Ziegler, T. *J. Comput. Chem.* **2001**, *22*, 931−967.
(26) Guerra, C. F.; Snijders, J. G.; te Velde, G.; Baerends, E. J. *Theor. Chem. Acc.* **1998**, *99*, 391−403.
(27) Vosko, S. H.; Wilk, L.; Nusair, M.; *Can. J. Phys.* **1980**, *58*, 1200−1211.
(28) Becke, A. D. *Phys. Rev. A* **1988**, *38*, 3098−3100.
(29) (a) Perdew, J. P. *Phys. Rev. B* **1986**, *34*, 7406−7406. (b) Perdew, J. P. *Phys. Rev. B* **1986**, *33*, 8822−8824.
(30) van Lenthe, E.; Baerends, E. J.; Snijders, J. *J. Chem. Phys.* **1993**, *99*, 4597.
(31) van Lenthe, E.; Baerends, E. J.; Snijders, J. *J. Chem. Phys.* **1994**, *101*, 9783.

Scheme 2

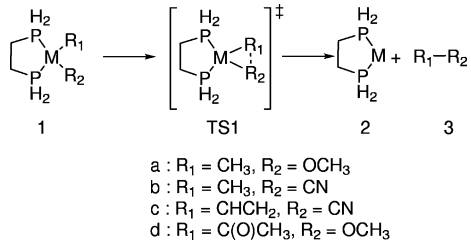

istic frozen-core potential was used, including 3d for palladium, 2p for phosphorus, and 1s for carbon, nitrogen and oxygen. A general numerical integration parameter of 6.0 was employed in all calculations. The QM/MM calculations were performed in ADF, using the IMOMM method developed by Maseras and Morokuma[33] and implemented by Woo et al.[34] The QM part consisted of the previously optimized model complexes, while the MM part, consisting of the substituents on the diphosphine ligands, was described using the SYBYL (Tripos 5.2) force field,[35] which was modified to include the van der Waals radius for palladium taken from the UFF force field.[36] Hydrogen was chosen as link atom, and the link bond parameter was set to 1.27 for the phenyl-substituted ligands and 1.29 for the methyl-substituted ligands. A simple electrostatic coupling model was employed, not allowing polarization of the QM wave function by the MM part of the calculation.

3. Results and Discussion

3.1. Substrate Effects. The reductive elimination of the XY moiety from model complexes $(H_2P(CH_2)_2PH_2)$-PdXY was considered first, aiming to isolate and evaluate the effect of the substrate on the reaction rate. The use of a model ligand bearing H substituents instead of phenyl groups, as in real-life complexes, is obviously a drastic simplification that affects both phosphine basicity and bulkiness. Indeed, several authors[37] reported conclusive evidence concerning the distinct electronic properties of PH_3 and triphenylphosphine ligands. In this paper, we will show that these kinds of model ligands are not able to reproduce subtle electronic effects. However, given that in this section we seek to analyze the behavior of different substrates, keeping frozen all other factors, these model systems seem appropriate. Additionally, they lack any steric influence and keep the original backbone, which retains the plasticity of the ligand along the reaction path, thus ensuring a proper description of the ligand bite angle.

Four cases, shown in Scheme 2, which correspond to the elimination of dimethyl ether, acetonitrile, vinyl cyanide, and methyl ethanoate, respectively, were considered. The corresponding reactants, products, and transition-state (TS) structures were fully optimized and the TSs fully characterized. The reaction energy (ΔE_{react}) and activation energy ($\Delta E^{\ddagger}$) for the reactions shown in Scheme 2 are given in Table 1. Clearly, large differences are observed in both the reaction energy and the activation energy of the four reactions.

Table 1. Reaction (ΔE_{react}) and Activation Energies ($\Delta E^{\ddagger}$) for 1a−d

	R_1	R_2	ΔE_{react}	$\Delta E^{\ddagger}$
1a	CH_3	OCH_3	4.7	38.0
1b	CH_3	CN	8.2	21.3
1c	$CH{=}CH_2$	CN	8.4	12.4
1d	$C(O)CH_3$	OCH_3	−8.8	0.0

[a] Energies are given in kcal mol^{-1}.

For the reductive elimination of dimethyl ether (**1a**) a large energy barrier (38.0 kcal mol^{-1}) was calculated. In light of this result, it is not surprising that few experimental studies have shown selective formation of dialkyl ethers catalyzed by palladium. In **1b**, the activation energy amounts to 21.3 kcal mol^{-1} for the reductive elimination of acetonitrile, a value that is in good agreement with the experimentally observed activation enthalpy for similar systems reported by Moloy and co-workers.[21] Changing the methyl group to a vinyl group (**1c**) lowers the activation barrier by 9 kcal mol^{-1}. The barrier for the reductive elimination of methyl ethanoate from complex **1d**, a proposed intermediate in the palladium-catalyzed methoxycarbonylation reaction, is extremely low. This explains why this complex has never been observed experimentally, despite extensive studies into this industrially important process.[38−40,22] Activation energies for systems **1b** and **1c** compare fairly well to similar systems reported recently by Ananikov,[24] but reaction energies differ substantially. The reason for this discrepancy arises from the distinct phosphine models considered in both studies. In the present case, we considered a diphosphine that keeps a bite angle close to 90° during the reaction; therefore, a diphosphine does not stabilize the Pd(0) product to the same extent as do two monophosphines. Indeed, the most stable geometry for a $(PH_3)_2Pd$ complex is linear.

The geometries of the reactants **1** and transition states **TS1** are shown in Figure 1. As was observed by Macgregor and co-workers, the reactions exhibiting high activation energies show significant geometric deformations in the transition state relative to the reactant.[15] Both methyl-containing complexes **TS1a** and **TS1b** show elongation of the palladium−methyl bond and bending of the methyl moiety toward the organic fragment. This is indicative of a partial breaking of the palladium−methyl bond in the transition state. In complex **TS1a**, also the palladium−methoxy bond is elongated, indicating that the methoxy oxygen lone pair is also involved in the formation of the new C−O bond. In contrast, unsaturated moieties such as the cyano, vinyl, and acyl groups in complexes **TS1b**, **TS1c**, and **TS1d** show no significant bond elongation. The cyano and vinyl groups are bent relative to the reactant. These observations suggest that these groups can participate in the bond-forming process without significant loss of bonding to the palladium center.

(32) van Lenthe, E.; Ehlers, A.; Baerends, E. J. *J. Chem. Phys.* **1999**, *110*, 8943−8953.
(33) (a) Maseras, F.; Morokuma, K. *J. Comput. Chem*. **1995**, *16*, 1170−1179. (b) Maseras, F.; *Chem. Commun*. **2000**, 1821−1827.
(34) Woo, T.; Cavallo, L.; Ziegler, T. *Theor. Chem. Acc.* **1998**, *100*, 307.
(35) Clark, M., Cramer, R. D.; van Opdenbosch, N. *J. Comput. Chem.* **1989**, *10*, 982−1012. Singh, U. C.; Kollman, P. A. *J. Comput. Chem.* **1986**, *7*, 718−730.
(36) Rappe, A. K.; Casewit, C. J.; Colwell, K. S.; Goddard, W. A.; Skiff, W. M. *J. Am. Chem. Soc.* **1992**, *114*, 10024−10035.
(37) (a) Gonzalez-Banco, O.; Branchadell, V. *Organometallics* **1997**, *16*, 5556−5562. (b) Woska, D.; Prock, A.; Giering, W. P. *Organometallics* **2000**, *19*, 4629−4638. (c) Haberlen, O.; Rosch, N. *J. Phys. Chem*. **1993**, *97*, 4970−4073.
(38) Drent, E.; Budzelaar, P. H. M. *Chem. Rev.* **1996**, *96*, 663−681.
(39) Bianchini, C.; Lee, H.; Meli, A.; Oberhauser, W.; Peruzzini, M.; Vizza, F. *Organometallics* **2002**, *21*, 16−33.
(40) van Leeuwen, P. W. N. M.; Zuideveld, M. A.; Swennenhuis, B. H. G.; Freixa, Z.; Kamer, P. C. J.; Goubitz, K.; Fraanje, J.; Lutz, M.; Spek, A. L. *J. Am. Chem. Soc.* **2003**, *125*, 5523−5539.

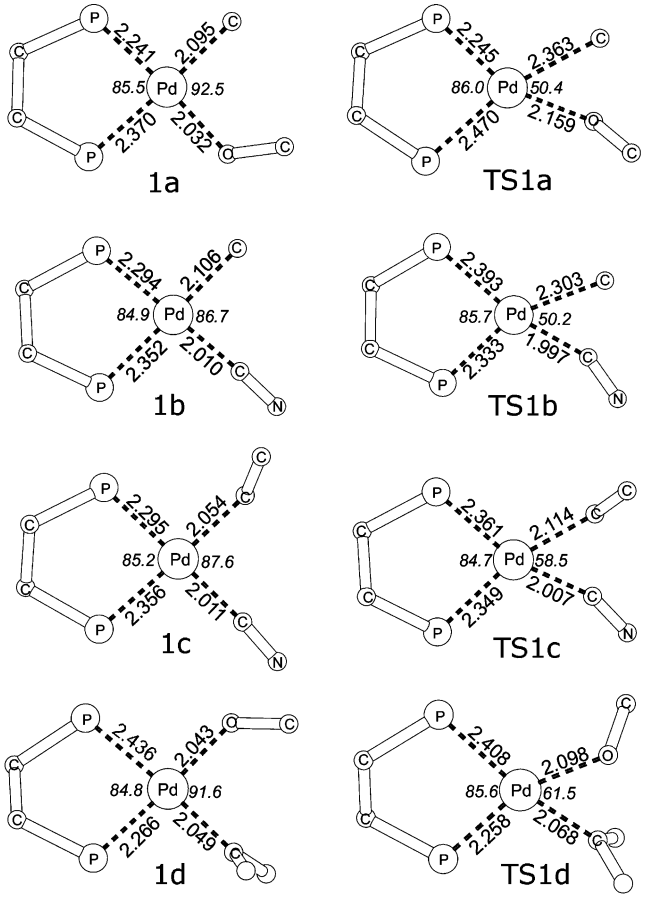

Figure 1. Selected geometrical parameters for reactants and transition states for **1a**−**d** (see Scheme 2). Hydrogen atoms have been omitted for clarity. Distances are given in Å and angles in deg.

In the following we analyze in detail the changes in the molecular orbitals during the reaction. Figure 2 shows the filled frontier molecular orbitals of the reactants and TSs. In all cases, the formal oxidation state of palladium is Pd(II) d^8; hence, four metal orbitals are filled, namely d_{xy}, d_{yz}, d_{xz}, and d_{z^2}. The additional eight electrons are provided by the two phosphine ligands and by the two formally anionic X and Y moieties, which complete the square-planar 16-electron rule. Also, the lone pair of the methoxy oxygen atom and the two cyano π orbitals must be taken into account. Given that the two phosphine lone pairs lie at lower energies and are not directly involved in the reaction, Figure 2 shows seven MO levels in cases A and D and eight levels in case B. During the course of the reaction, the two X− and Y−metal σ bonds break, a new X−Y bond forms, and two electrons are transferred into the empty $d_{x^2-y^2}$ orbital, thus forming Pd(0) d^{10}. As soon as X and Y approach one another, the overlap between the two filled X and Y orbitals increases, and bonding and antibonding combinations of both orbitals are developed. The bonding combination has the proper symmetry to interact with d_{xy} and/or d_{z^2}, while the antibonding combination overlaps effectively with the empty $d_{x^2-y^2}$. The energetic cost of this electronic rearrangement depends strongly on the relative energy of orbitals involved in the reaction and, thus, on the electronic nature of X and Y.

In the elimination process of methyl ethanoate, case D in Figure 2, the filled metal orbitals are clearly identified and located in the low-energy region. The remaining three MOs contain the metal−ligand σ bonds, the methoxy lone pair being the HOMO. In all cases, the d_{z^2} level remains unchanged during the reaction while the energy levels of out-of-plane d_{yz} and d_{xz} rise. The metal−σ bonds build up by mixing the ligand orbitals with the in-plane metal orbitals. In case D, the reduction process is clearly visible as an electron flow into $d_{x^2-y^2}$ (HOMO-2 in the TS). As mentioned before, the methoxy moiety rotates along the Pd−O bond in order to orient the oxygen lone pair toward the acyl group and participate in the bond forming process while the σ oxygen electrons mix with $d_{x^2-y^2}$. In this case, no significant deformation of the two reacting moieties is observed in the transition state. Already in the reactant, significant overlap between the filled lone pair on the methoxy species and the empty π^* orbital of the acyl species is observed, resulting in an effective donor−acceptor type bond-forming process. Indeed, the three orbitals involved in the reaction are stabilized in the TS; thus, no significant amount of energy is required.

In the elimination reaction of dimethyl ether, case A in Figure 2, metal orbitals appear at higher energies than they do in case D. This is due to the better donor properties of the methyl ligand, which promotes a higher electron density on the metal. Note how the methyl electrons appear at lower energies than the acyl electrons in case D, while the methoxy orbitals lie at similar energies. As mentioned above, strong geometric deformations are observed in the methyl−palladium bond, which is reflected in Figure 2 by the energy increase of all orbitals involved in the reaction, representing an electronic reorganization that requires a considerable amount of energy. Note also in this case that the methoxy moiety rotates along the O−Pd bond in order to enhance the overlap between the methoxy oxygen lone pair and the methyl. However, in this case this interaction is repulsive, because the methyl moiety displays null acceptor capabilities.

When the methoxy group is substituted by a cyano ligand, case B, a different picture emerges. The HOMO is the metal d_{z^2}, because the cyano ligand is more basic than a methoxy ligand and the cyano orbitals lie at lower energies. In the TS, a strong mixing of the σ and π in-plane cyano orbitals is observed, as reflected in Figure 2. This can be attributed to a rehybridization of the cyano orbitals, which generates an additional orbital to participate in the bond formation process without significantly decreasing the ability of the group to bind to palladium, similar to the methoxy lone pair in case D. The π_{CN} orbital perpendicular to the plane of the complex (second lowest level in Figure 2B) remains unchanged during the reaction. However, the in-plane π_{CN} system of the cyano group contributes to the formation of the new carbon−carbon bond. Note that the difference in energy between orbitals involved is smaller than that in case A; thus, the electronic reorganization requires less energy cost in case B than in case A.

3.2. Bite Angle Effects. We used the following computational strategy to isolate and evaluate electronic and steric effects. To assess the electronic bite angle effect in the absence of steric bulk, DFT calculations were performed on the model system (H_2PXPH_2)Pd-

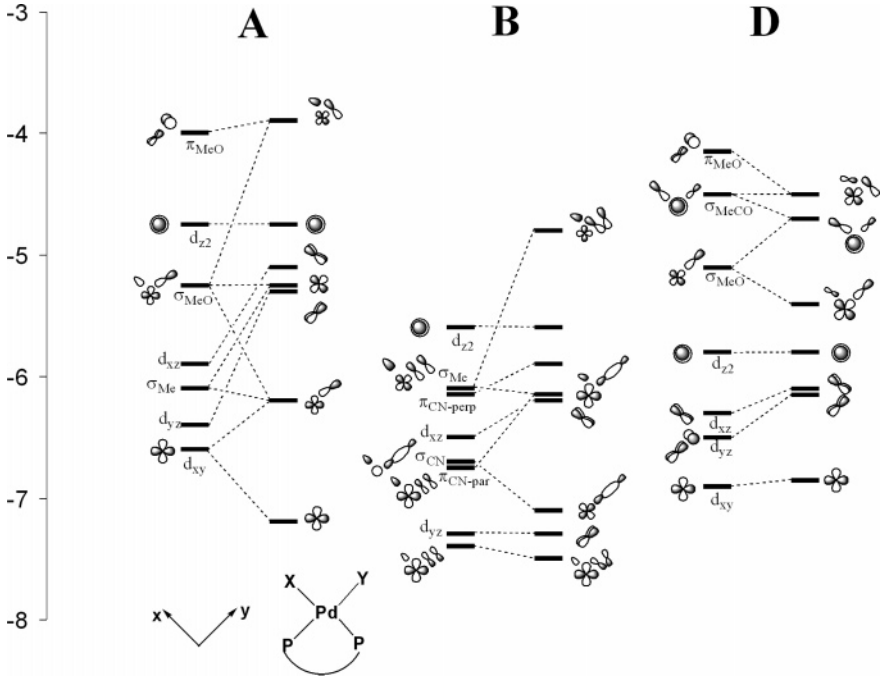

Figure 2. Correlation diagram between filled frontier molecular orbitals for the reactant (left) and for the TS (right), corresponding to the elimination of (A) dimethyl ether, (B) acetonitrile, and (D) methyl ethanoate.

$(CH_3)(CN)$ for a number of different ligand backbones (X = $(CH_2)_n$, n = 1−4; X = *cis*-, *trans*-but-2-ene) spanning a large bite angle range. Next, realistic substituents were introduced by substituting both of the hydrogen atoms in the phosphine with methyl and phenyl groups. Phenyl- and methyl-substituted systems were investigated using a QM/MM methodology, treating the substituents at the MM level, while calculating the remainder of the molecule at the QM level. Because the part of the complex included in the QM partition remains constant throughout these calculations, comparison between the model system H_2PXPH_2 and the more realistic systems is straightforward. Energy differences between the model structures and the QM part of the QM/MM structures arise from steric deformation of the central part of the molecule by the bulky substituents of the realistic ligand systems, while the MM energy gives an estimate of the steric repulsion between the ligand and the reacting moieties. In the final step the QM/MM optimized structures were subjected to single-point DFT calculations in order to include electronic and steric effects and to assess the effect of ligand basicity on the energy barrier.

(a) Model System. Figure 3 shows the calculated structures for model complexes **3**, **4**, and **TS3**, including some geometric parameters. Both the reactants **3** and the transition states **TS3** are very similar for all ligands. The transition state is asymmetric and resembles the transition state of the migratory insertion of carbon monoxide into a palladium−alkyl bond calculated by Ziegler and co-workers.[41] The process of migratory reductive elimination was already suggested in a theoretical study by Calhorda et al.[11] for unsymmetrical substrate combinations and was proposed by Marcone and Moloy for the reductive elimination of nitriles from palladium, on the basis of the isoelectronic relationship between CO and CN^-.[21] Geometric differences between the different transition states are most pronounced in the bite angle (P−Pd−P angles) of the various complexes. Table 2 lists the P−Pd−P angles for the calculated structures as well as the reaction and activation energies. With the exception of the diphosphinomethane ligand in complex **3a**, all ligands are able to accommodate a P−Pd−P angle of approximately 90° in the square-planar reactant **3**. As expected, the P−Pd−P angle increases during the reaction for all six ligands in order to stabilize the final Pd(0) species **4**. The changes in the angle on going from **3** to **TS3** are small, though, and it only increases significantly beyond the transition state.

A clear trend in reaction energy is observed in Table 2. This trend correlates well with the ability of the ligand to stabilize the final Pd(0) species **4** by adopting a larger P−Pd−P angle during the reaction. Diphosphinomethane falls outside this correlation, which can be attributed to an electronic destabilization of the square-planar reactant caused by the extremely small natural bite angle of this ligand.[19] This is also illustrated by the lower activation energy for this ligand. It should be noted that it has been shown experimentally that this methane backbone tends to induce the formation of dimeric structures,[42] thus avoiding the formation of high-energy mononuclear Pd(II) species.

Excluding the diphosphinomethane ligand, the differences in the activation energies of the different model complexes are small. Interestingly, the highest activation barrier is observed for the propane-based ligand, which has a natural bite angle of 91° and is therefore best suited to stabilize the square-planar reactant. Ligands that exhibit a natural bite angle that significantly differs from 90°, such as the methane- and *trans*-2-butene-bridged ligands, yield significantly lower activation energies due to electronic destabilization of the

(41) Margl, P.; Ziegler, T. *J. Am. Chem. Soc.* **1996**, *118*, 7337−7344.

(42) Reid, S. M.; Mague, J. T.; Fink, M. J. *J. Am. Chem. Soc.* **2001**, *123*, 4081−4082.

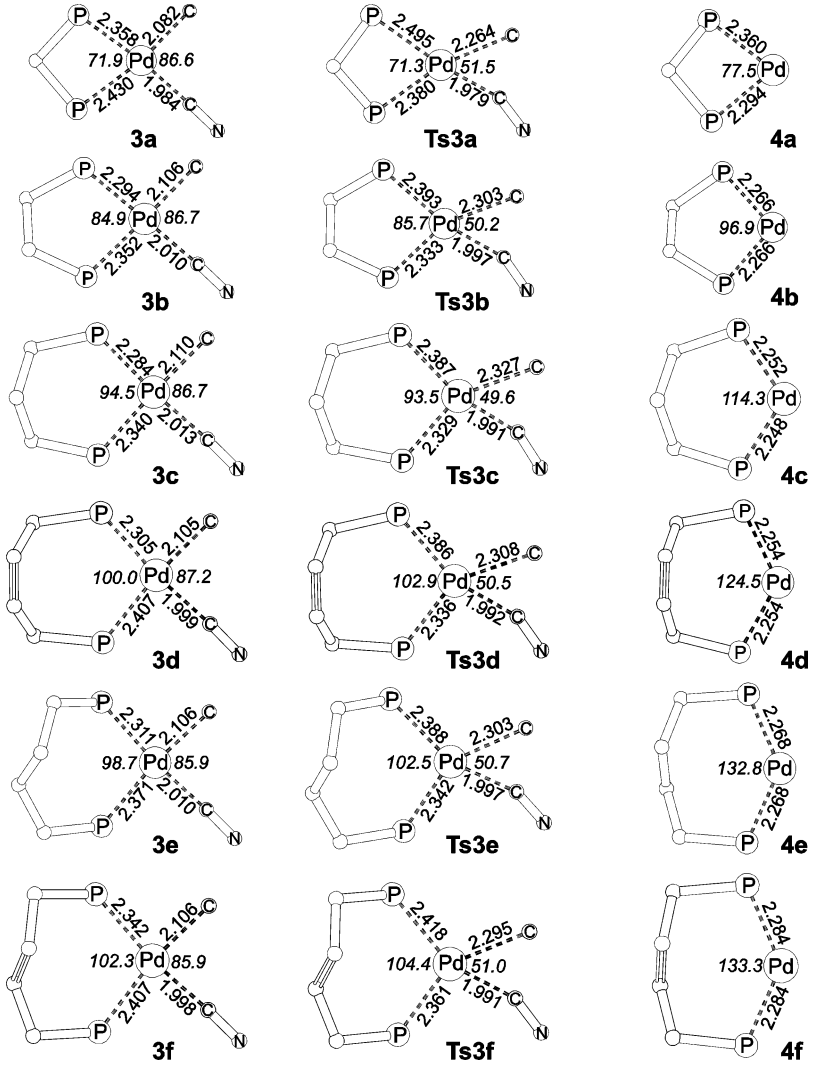

Figure 3. Geometries of model complexes **3**, **TS3**, and **4**: top view along the perpendicular axis to the square-planar plane. Hydrogen atoms have been omitted for clarity. Distances are given in Å and angles in deg.

Table 2. Bite Angles (P−Pd−P) and Activation and Reaction Energies[a]

	bite angle				
n	**3**	**TS3**	**4**	$\Delta E^{\ddagger}$	ΔE_{react}
$-CH_2-$	71.9	71.3	77.5	17.8	6.0
$-C_2H_4-$	84.9	85.7	96.6	21.3	8.2
$-C_3H_6-$	94.5	93.5	113.4	22.0	6.2
$-C_4H_6-$ (cis)	100.0	102.9	124.4	21.8	2.1
$-C_4H_8-$	98.7	102.5	132.8	21.0	1.3
$-C_4H_6-$ (trans)	102.9	104.3	133.3	19.6	−3.1

[a] Bite angles are given in deg, and energies are given in kcal mol^{-1}.

Table 3. Decomposition of the Activation Energies for QM/MM Structures[a]

	methyl			phenyl		
backbone	QM	MM	total	QM	MM	total
$-CH_2-$	17.9	0.8	18.6	18.1	0.2	18.3
$-C_2H_4-$	21.4	0.9	22.3	21.6	1.2	22.8
$-C_3H_6-$	22.2	0.3	22.5	21.9	0.4	22.4
$-C_4H_6-$ (cis)	21.9	0.3	22.2	22.0	0.4	22.4
$-C_4H_8-$	21.0	−0.2	20.9	21.0	−0.6	20.4
$-C_4H_6-$ (trans)	19.5	0.0	19.5	19.7	0.6	20.3

[a] Energies are given in kcal mol^{-1}.

reactant: i.e., an electronic bite angle effect. However, using these model systems, the experimental trend observed by Moloy and co-workers is not reproduced. Indeed, Table 3 shows that model systems predicted higher activation energy for the propane than for the *cis*-2-butene.

(b) Steric Effects. The activation energies computed at the QM/MM level for methyl- and phenyl-substituted systems are shown in Table 3. The methyl-substituted system exhibits the same trend in total energy as the model system. This result indicates that the methyl substituents do not induce a significant amount of steric strain and, therefore, do not influence the reaction rate. The more bulky phenyl substituents do yield a small change in $\Delta E^{\ddagger}$. Decomposing this activation energy into its QM and MM contributions, it becomes clear that the MM contributions to the overall energy barrier are small for all ligands and are very similar for methyl- and phenyl-substituted ligands. Furthermore, the MM contribution is positive in most cases, which clearly contradicts the notion that for these ligands the reaction rate is enhanced by the alleviation of steric repulsion during the reaction.

The QM contribution of both the methyl- and phenyl-substituted complexes can directly be compared to the energy of the corresponding model complexes listed in Table 2. The small energy differences between the QM

Table 4. Deformation Energies Caused by Steric Effects[a]

	methyl			phenyl		
backbone	**5**	**TS4**	**6**	**7**	**TS5**	**8**
$-CH_2-$	0.3	0.4	0.6	0.7	1.0	1.6
$-C_2H_4-$	0.2	0.3	0.6	1.8	2.1	2.4
$-C_3H_6-$	0.5	0.5	0.6	2.8	2.6	2.0
$-C_4H_6-$ (cis)	0.3	0.4	0.5	0.7	0.8	1.2
$-C_4H_8-$	0.7	0.7	0.6	3.2	3.2	1.5
$-C_4H_6-$ (trans)	0.4	0.4	0.4	1.5	1.7	2.3

[a] Computed as the QM energy of QM/MM geometry optimized for a realistic system minus the QM energy of a model system. All values are given in kcal mol^{-1}.

Table 5. QM Energies at the QM/MM Optimized Structures for Methyl- and Phenyl-Substituted Ligands[a]

	ΔE_{react}			$\Delta E^{\ddagger}$		
backbone	H	methyl	phenyl	H	methyl	phenyl
$-CH_2-$	6.0	17.2	16.5	17.8	22.8	22.5
$-C_2H_4-$	8.2	17.9	13.9	21.3	26.2	25.4
$-C_3H_6-$	6.2	14.0	8.7	22.0	26.0	23.2
$-C_4H_6-$ (cis)	2.1	8.7	2.7	21.8	24.4	22.3
$-C_4H_8-$	1.3	5.3	−6.4	21.0	22.4	20.5
$-C_4H_6-$ (trans)	−3.1	1.9	−4.3	19.6	21.3	19.3

[a]Values for hydrogen-substituted ligands are included for comparison. All values are given in kcal mol^{-1}.

parts of the QM/MM methyl- and phenyl-substituted systems and the model system suggest that the steric deformation of the central part of the complex is rather small for all ligands or that both the reactant and the transition state are deformed in a similar fashion by the steric bulk. Table 4 shows the deformation energies of all methyl- and phenyl-substituted complexes. Indeed, for the more bulky phenyl group, the deformation energy increases as the bite angle of the ligand increases, but the deformation energies of the reactant and transition state are similar for all ligands, negating any effects on the overall activation barrier of the reaction. Therefore, steric effects do not play an important role in determining the rate of elimination for the ligands studied here and the ligands studied experimentally by Marcone and Moloy.[21]

(c) Electronic Effects. When single-point energy calculations were applied to the QM/MM optimized structures, realistic reaction and activation energies were finally obtained. Along with the energies of the model system, these are listed in Table 5.

In general, the increased basicity of the ligands containing phenyl and methyl substituents relative to the hydrogen-substituted ligands leads to an increase in the activation energy. The highest activation energies are obtained for the methyl-substituted ligands. A bite angle trend resembling the experimentally observed trend is clearly found in the activation energy for both the methyl- and phenyl-substituted ligands. For the hydrogen-substituted model ligands, the trend is much smaller (vide infra). Increasing the bite angle leads to a lowering of the activation energy for the reductive elimination. On the basis of the observations on the QM/MM energies and the absence of large energy differences between phenyl-substituted ligands and the much less bulky methyl-substituted ligands at the DFT level here, the observed trend must be attributed to an electronic bite angle effect.

Table 6. Phosphine−Metal Fragment Interaction Energies for Reactants (ΔE_{int}^{R}), TS (ΔE_{int}^{TS}), and the Difference $\Delta\Delta E_{int}$ for R = Me

n	ΔE_{int}^{R}	ΔE_{int}^{TS}	$\Delta\Delta E_{int}$
$-CH_2-$	−68.7	−55.4	−13.3
$-C_2H_4-$	−108.7	−64.3	−21.6
$-C_3H_6-$	−107.6	−65.5	−17.8
$-C_4H_6-$ (cis)	−103.3	−65.7	−13.5
$-C_4H_8-$	−98.9	−67.1	−12.4
$-C_4H_6-$ (trans)	−93.6	−64.2	−9.9

[a]All values are given in kcal mol^{-1}.

Table 7. Decomposition of Metal−Ligand Interaction Energy for R = Me[a]

	reactant			TS		
n	ΔE_{Pauli}	ΔE_{elstat}	ΔE_{orb}	ΔE_{Pauli}	ΔE_{elstat}	ΔE_{orb}
$-CH_2-$	183.4	−164.2	−87.9	148.4	−138.1	−65.8
$-C_2H_4-$	225.5	−202.7	−108.7	196.9	−182.7	−78.4
$-C_3H_6-$	225.0	−200.7	−107.6	205.4	−189.5	−81.4
$-C_4H_6-$ (cis)	217.6	−193.5	−103.3	208.3	−192.4	−81.6
$-C_4H_8-$	203.5	−184.1	−98.9	209.3	−194.5	−81.9
$-C_4H_6-$ (trans)	190.1	−170.7	−93.6	195.9	−180.9	−79.1

[a] All values are given in kcal mol^{-1}.

To investigate this trend in more detail, the methyl-substituted ligand system was analyzed using the ETS energy decomposition scheme developed by Ziegler and Rauk.[43] We were especially interested in the interaction between the ligand and the metal fragment. The interaction energies (ΔE_{int}) in the reactants and in the transition states for the methyl-substituted systems are listed in Table 6, together with the difference between ΔE_{int} on going from the reactant to the transition state ($\Delta\Delta E_{int}$).

On comparison of the different ligands, ΔE_{int} can be considered to be a measure for the stability of the complex. As expected for the (square-planar) reactant, the optimal interaction is observed for the ethanediyl and propanediyl-bridged ligands, while ligands that induce bite angles which differ significantly from 90° destabilize the metal−ligand interaction and therefore the reactant. In the transition state, a different trend is observed. Here the butane-based ligand, with a bite angle of 103°, stabilizes the complex most effectively. In essence, the optimal stabilization shifts to a wider bite angle during the reaction. These two trends point in the same direction, and combined, they are responsible for the observed bite angle trend in Table 6. This is illustrated in the change in interaction energy during the reaction $\Delta\Delta E_{int}$, which follows the same trend as the activation energy for the reaction. Interestingly, the methyl-bridged ligand which induces a very small bite angle shows extensive destabilization of both the reactant and the transition state, leading to only a small value for $\Delta\Delta E_{int}$ and a low activation barrier.

The ETS analysis allows us to divide the interaction energy ΔE_{int} into three separate components: the Pauli repulsion ΔE_{Pauli}, the electrostatic interaction energy ΔE_{elstat}, and the orbital interaction energy ΔE_{orb}. The individual contributions to ΔE_{int} for both the reactant and the transition state for the methyl substituted system are given in Table 7. From the decomposition of ΔE_{int} it becomes clear that there is a significant orbital effect in both the stability of the reactant and the

(43) Ziegler, T.; Rauk, A. *Theor. Chem. Acta* **1977**, *46*, 1−10.

transition state. ΔE_{orb} follows the same trends as the total interaction energy ΔE_{int}, which suggests that the observed bite angle trend in ΔE_{int} and the activation energy can be correlated to differences in orbital overlap between the organometallic fragment and different ligands. However, this orbital effect is accompanied by an electrostatic contribution which exhibits similar trends in the reactant and the transition state, suggesting that the orbital effect is not solely responsible for the bite angle trend in the activation energy. The Pauli repulsion energy term shows the opposite trend, the increase in orbital and electrostatic interaction between the two fragments also leading to an increase in the Pauli repulsion.

Although the energy decomposition gives some insight into the changes we observe in the reaction energies, there is not a single contribution that accounts for the observed trend in ΔE_{int}. The values of ΔE_{orb} and ΔE_{elstat}, which in the literature are sometimes interpreted as the covalent and ionic contributions to the metal−ligand bond, both contribute to the interaction energy;[44,45] combined they account for the observed trend in ΔE_{int}. The trend in the activation energy can only be related directly to the change in ΔE_{int}. As the interaction energy is an important part of the bond dissociation energy, the observed bite angle trend can now be attributed to destabilization of the metal−ligand interaction in the square-planar reactant and stabilization of the transition state by the wide bite angle ligands.

4. Conclusions

From the results and analysis presented above, we can draw the following conclusions.

(i) Energy barriers for reductive elimination in palladium diphosphine complexes depend largely on the electronic nature of substrates and, to a lesser extent, on the phosphine ligand properties. A null energy barrier was computed for the elimination of methyl ethanoate and moderate energy barriers were obtained for the elimination of acetonitrile and vinyl cyanide, while the largest barrier was found for dimethyl ether elimination. These results are in very good agreement with experimental findings and with previous computational studies on related systems.

(ii) Molecular orbital analysis clearly revealed that donor/acceptor capabilities of the substrates determine the energetic cost required for electronic reorganization. Orbital energies reflect clearly the nature of reactant moieties and its effect on the metal. The lowest barrier is obtained when metal orbitals lie at low energies, hence more electrophilic character, and when ligand orbitals appear above. It seems that the combination of these two factors facilitates electron transfer from ligands to the metal, thus reducing the metal formal oxidation state.

(iii) For the elimination of acetonitrile, the results we obtained reproduce fairly well the reaction rate dependence on the diphosphine ligand bite angle found in Moloy's experiments. Although the QM/MM model phosphines reproduce the geometry of the complexes accurately, they fail to reproduce the electronic properties of real ligands and, therefore, the trend in the activation energy. The lack of electrostatic coupling between the QM and MM partitions prevents the proper description of phosphine electronic properties at the QM/MM level. Since the two phosphorus ligand lone pairs interact with in-plane palladium electrons that are directly involved in the reaction and since these electrons are also sensitive to the bite angle of the ligand, both the phosphine basicity and the electronic bite angle effect are transferred to the reactant moieties through the metal using the same metal orbitals. Therefore, there is no error compensation and both effects must be properly included. This was finally achieved when we treated the full system at the DFT level.

(iv) QM/MM strategies were used to separate and evaluate the steric and the electronic contributions to the activation energy. No purely steric effects were characterized, and consequently, relief of steric strain could not be assigned to the energy barrier lowering.

(v) On the contrary, as was suggested some time ago[46] when wide bite angle ligands were successfully applied in the hydrocyanation reaction, metal−ligand interaction energies computed in this study demonstrated that the origin of the activation energy lowering when the ligand bite angle increases must be attributed to electronic bite angle effects; the largest bite angle gives the least stable reactant and the most stable transition state, and thus the lowest barrier is obtained.

Acknowledgment. This work was supported (E.Z.) by the Council for Chemical Sciences of The Netherlands Organization for Scientific Research (CW-NWO). We are indebted to the MCYT of the Government of Spain (BQU2002-04110-C02-02), to the CIRIT of the Catalan Government (SGR01-00315), and to the ICIQ Foundation for financial support. We acknowledge the SARA Center for High-Performance Computing for use of their computational facilities.

OM050113X

(44) Diefenbach, A.; Bickelhaupt, F. M.; Frenking, G. *J. Am. Chem. Soc.* **2000**, *122*, 6449−6463.
(45) Brust, D. J.; Gilbert, T. M. *Inorg. Chem.* **2004**, *43*, 1116−1121.
(46) Kranenburg, M.; Kamer, P. C. J.; van Leeuwen, P. W. N. M.; Vogt, D.; Keim, W. *J. Chem. Soc., Chem. Commun.* **1995**, 2177−2178.